BBC
BROWN BOVERI

Last-Stage Blades of Large Steam Turbines

Publication No. CH-T 060040 E

A. Hohn and P. Novacek

The present article deals with the blades in the last rotating row in large steam turbines, considering them as a machine element. The static and dynamic stresses occurring in service are discussed and their effect on the design of the blades is demonstrated. Some methods of testing which are used in the design of prototypes are explained as they enable blades designed on pure theory to be tested under conditions comparable with those experienced in service, thereby enabling the behaviour of the blades in service to be predicted. Nowadays this performance is from time to time checked in service in power stations; the article provides some information regarding test procedures and the results obtained. In conclusion the authors discuss future developments in blade construction.

Introduction

A feature of the last ten years in the construction of steam turbines was the marked rise in the unit ratings of machines. At the beginning of the 1960's the majority of large thermal machines in European installations were mainly in the 125 to 150 MW range. Today, both in Europe and in America, machines with an output of more than 1000 MW are being installed. In them the volume of steam that has to be handled on emerging from the blading (last-stage) may be of the order of magnitude of 10000 m³/s (fossil fuelled plants) up to 25000 m³/s (in nuclear power plants with turbines employing saturated steam). In order to handle such enormous quantities of steam in a reasonable number of flows, the cross-section of flow in the blade ducts has to be large and the last stage correspondingly long. On the other hand, in the last row of blades of large steam turbines about 6% of the total heat drop of the steam flowing through the turbine is converted into mechanical energy. Since these two factors—high output and quality of the energy conversion—are also influenced by the last stage, particular attention has been paid to these blades during the past ten years. Here, developments in computer applications proved of great assistance to the engineers concerned with strength and flow problems. On the one hand, the blade angles and profiles had to be determined with the aid of a three-dimensional flow calculation; on the other hand, the aptitude of the twisted last-stage blades had to be proved under service conditions.

The cost of producing the last-stage blades for large turbines is high. Therefore, the turbine manufacturers endeavour to market a product which will perform its duties without any trouble for many years.

Comparing new designs of last-stage blades with those of the past, it is strikingly evident that mechanically sound designs today dispense with forms of "aids to survival". Damping wires and in some cases cover strips are now a thing of the past for large turbines running at constant speed.

Apart from reducing costs and obtaining a better efficiency by this means, the machine is also made more reliable because the unsupported blade is mounted under very definite conditions which makes calculation simpler. Furthermore, with the methods of measuring now available the results obtained by calculation can easily be checked and calibrated in service.

Static Stresses of the Blade

The cross-section of a blade varies considerably from bottom to top, the main axis of inertia of the individual cross-sections being twisted from one to another as can be seen in Fig. 1 and 2.

The path taken by development can be seen in Fig. 3 where a blade used forty years ago for a speed of 1200 rev/min, which was slightly tapered and hardly twisted at all, is compared with a modern type of blade from a 400 MW (3000 rev/min) turbine. What is most striking is the difference in the shape of the cross-sections along the radius in the two designs.

Since the centrifugal stress σ_z (see Table I) is responsible for the greater part of the total stress, even in twisted blades (Fig. 4), it may be adopted as a rough guide to the cross-section of the blade. Using the notation from Fig. 4 we then obtain:

Differential centrifugal force

$$dK = -\varrho r\omega^2 F(r)\, dr \qquad (1)$$

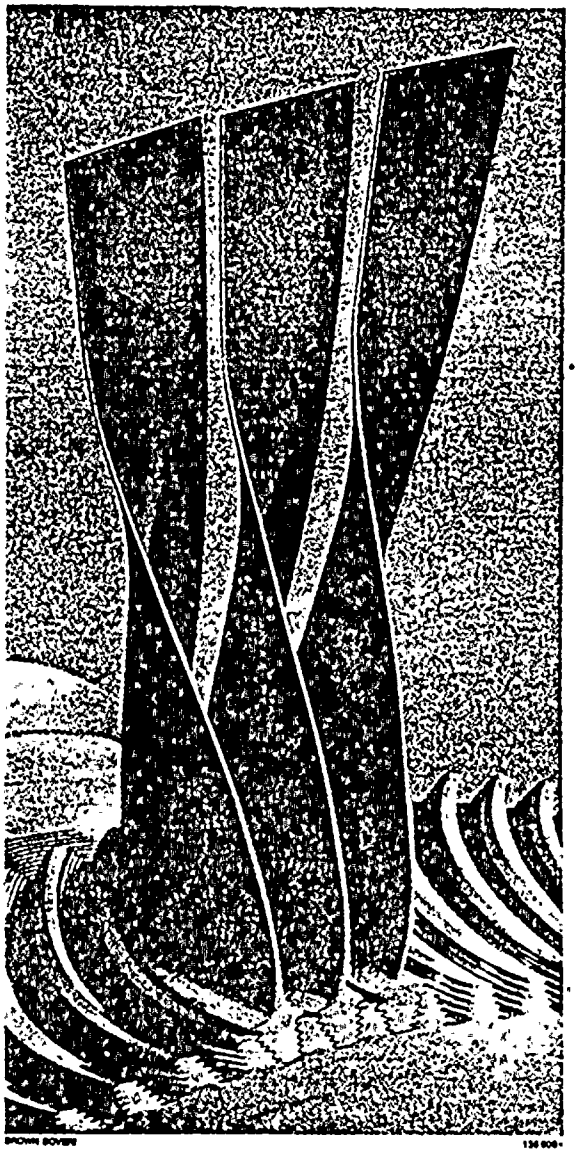

Fig. 1 – Last-stage blades of a 600 MW turbine in the assembled state

Local blade stress

$$\sigma_z = -\frac{\int_{R_2}^{R} \varrho r\omega^2 F(r)\,dr}{F(R)} \qquad (2)$$

If $F(r) = F$ is constant, as was approximately the case in the older blades illustrated in Fig. 3, the relationship between the tension due to centrifugal force in terms of the radius is given by

$$\sigma_z = \frac{\varrho\omega^2}{2}(R_2^2 - r^2) \qquad (3)$$

The stress in the blade in this case increases quadratically from the tip to the base and attains its maximum value in the transition from blade to root (Fig. 5). With this shaping the designer has not made the best use of the materials and the attainable peripheral speeds therefore remain considerably below those of tapered blades. If on the other hand, an attempt is made to keep the tensile stress due to centrifugal force constant over the greater part of the length of the blade by differentiating equation (2)

$$\frac{dF(r)}{F(r)} = -\frac{\varrho\omega^2}{\sigma_z} r\,dr \qquad (4)$$

the following solution is obtained:

$$F(r) = F_1 e^{\frac{\varrho\omega^2}{2\sigma_z}(R^{*2} - r^2)} \qquad (5)$$

Modern last-stage blades have a cross-section which roughly complies with equation (5) (see Fig. 4): σ_z is almost constant along the length of the blade. From equation (5) it is apparent that the variation in cross-section of the blade is only dependent on the material chosen (ϱ, σ_z), the speed (ω) and the geometry (R^*, r). This situation is illustrated in Fig. 6 for the blade according to Fig. 2 made from three different materials.

In service, however, these blades are also subjected to other stresses besides σ_z (Table I):

– Due to inaccuracy in manufacture or due to deliberate deviation of the line connecting the centres of gravity of the various cross-sections from the radial, the blade is subjected to bending due to centrifugal force (σ_B), which may be added to or subtracted from σ_z according to its sign.

In the older designs (cylindrical blades) σ_z and σ_B are the sole stress components produced in the blade by rotation. Consequently, calculation of the stresses due to rotation is easy for such blades and can be readily analysed.

– In modern, long, last-stage blades, however, apart from the change in profile down the length of the blade, the

Table I: Stresses in the twisted last-stage blades of turbines in service

	Type of stress	Cause
Static	1 Constant tension due to centrifugal force σ_Z	Centrifugal force produced by the blade mass situated above the given cross section
	2 Flexural stress due to centrifugal force σ_B	The departure of the line joining the centre of gravity of the sections from the radial
	3 Untwisting normal stress σ_E	The twisting of the blade due to centrifugal force
	4 Untwisting sheer stress τ_E	The twisting of the blade due to centrifugal force
	5 Flexural stress due to steam force σ_D	Steam force acting on the blade
Dynamic	6 Alternating flexural stresses σ_W	Steam flow deviations from the preceding stationary blading, detachment, asymmetry (disturbances) in the design (at the horizontal joint), disturbing internals such as probes, critical speeds, short circuit at the generator

Fig. 2 – Shape of profile and velocity triangles of a last-stage blade 1000 mm long

U = Peripheral speed
C_1 = Absolute velocity of the steam entering the blade

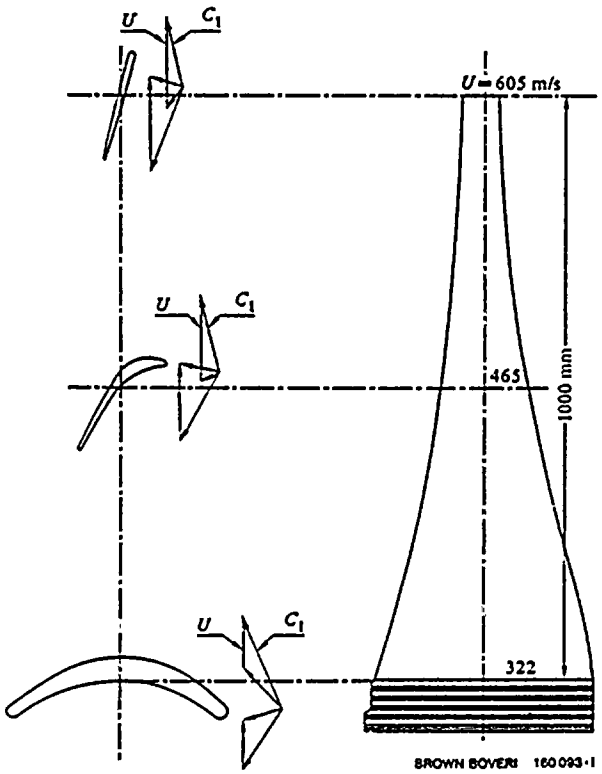

Fig. 3 – Comparison between last-stage blades as made in 1930 (n = 1200 rev/min) and in 1965 (n = 3000 rev/min)

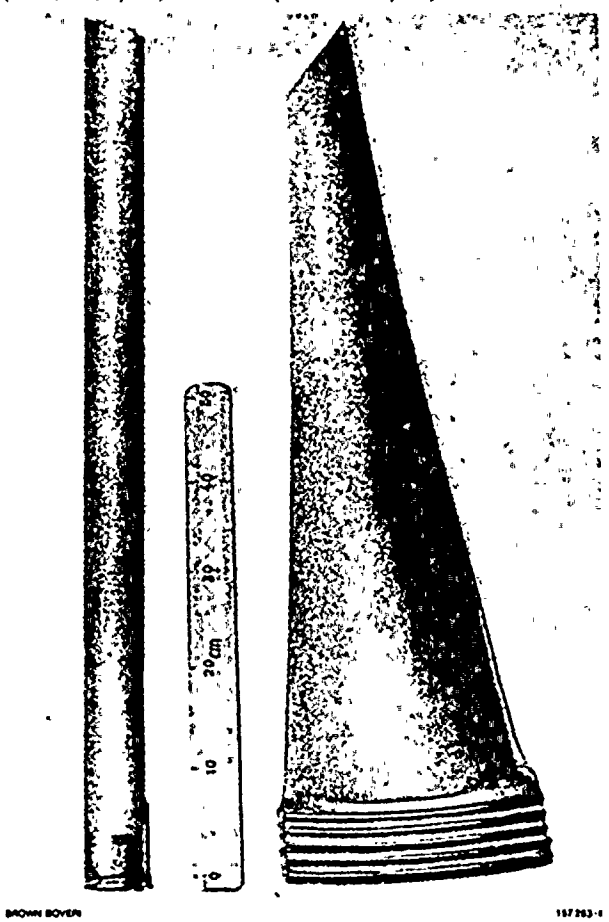

individual cross-sections are subjected to successive twist in order to allow for the change in peripheral speed over the height of the duct. Due to rotation of these blades, two additional stress components occur: the normal stress σ_E and the sheer stress τ_E due to the blade untwisting. A helpful model which shows how these stresses are produced can be seen in Fig. 7. This shows that when the blade untwists under the effect of a centrifugal force compression stresses are produced in the outer sections while the middle section is subjected to tension and torsion.

– Apart from these stress components produced by rotation the blade is also subjected to the forces produced by the flowing medium. Here a distinction must be made between the static component and a dynamic component of stress σ_W. Table I provides information about the causes leading to these stresses.

It is quite evident that for calculation of the stresses of the twisted tapered blade it is essential to use computers because the stresses 1 to 5 in Table I at different points on the edges of the profile have to be calculated for different cross-sections. Fig. 4 shows the result of such a stress calculation. Therein the reference stress σ_V = sum of the stress components, was determined according to the sheer stress hypothesis [1].

For practical applications it is extremely important to check the results of the stress calculations by random measurements, because when more is known about the stresses it is possible for optimum utilization of the material to be achieved. Here the following checks are possible.

– The stresses in the rotating blades are measured when the bladed rotor is overspeed tested. Groups of strain gauges are attached to the blade; the readings usually being transmitted to recorders by a system of sliprings.

– It is, of course, possible that the actual measurement of the blade stress cannot be undertaken because no means of transmitting the measurement can be attached to the rotating rotor. Usually the employment of a slipring system to transmit the measurement requires drillings in the rotor body for the leads, which in turn results in undesired stress concentration. The use of a telemetry system also imposes certain restrictions on the geometry of the rotor which have to be taken into account when it is designed. Therefore, when direct stress measurement is not possible, for the reasons given, the blade fitted with strain gauges may be run up to overspeed in stages and after each run examined at standstill to check for local exceeding of the yield point by measuring the change in the electrical resistance of the strain gauge compared with the initial value. However, since this is only a means of calibrating the calculation, it is immaterial whether the blade consists of low-alloy annealed material.

– A further check is to measure the angle of plastic untwist. Whereas long last-stage blades untwist elastically in service by between 5 to 8°, under experimental conditions the blades can be brought to such peripheral speeds that plastic untwist occurs to an extent that can be measured. By extrapolation to zero plastification the speed can be determined at which the blade "still just" remains elastic. The speed determined in this way at which plastification begins represents the upper limit at which the test blade may be used and from the relationship

$$\sigma \sim n^2 \qquad (6)$$

is also applicable to blades having the same geometry but other strength values.

Fig. 4 – Distribution of the combined stress across the blade, showing the relationship between the sum σ_V of all stress components according to Table I to the maximum value $\sigma_{V\max}$

F_1 = Reference cross-section (see eq. 5)
R_1 = Hub radius
R_3 = Radius at the tip
R^* = Radius of the reference cross-section
r = Coordinates
σ_V = Reference stress
σ_Z = Tension due to centrifugal force

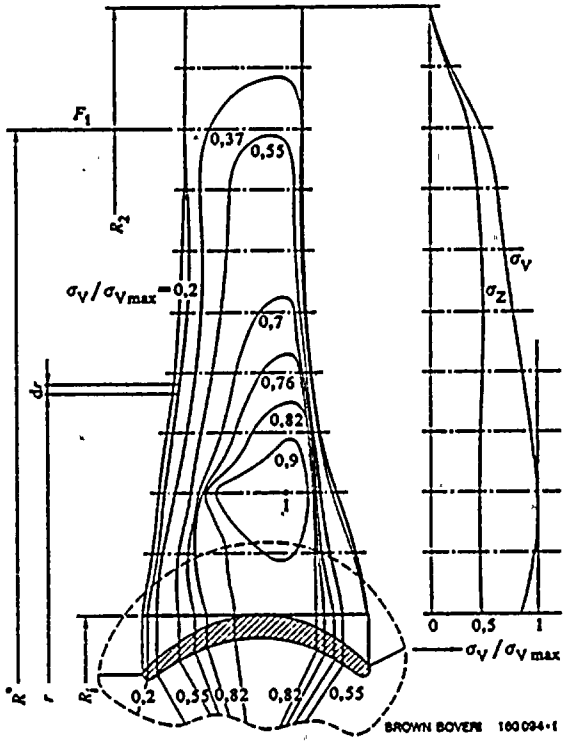

Attachment of the Blades to the Shaft

The blades of the last stage of large turbines develop centrifugal forces of some hundreds of tons when running. For this reason only very efficient methods of attachment can be considered. Among the systems in use at present, such as rhombus fixing in a peripheral slot, finger-shaped bolted fixing, straight or curved fir-tree roots, the last mentioned is an ideal means of attachment because it permits very close staggering of the blade cascade and the centrifugal force is produced in an optimum manner in the shaft teeth. This design is illustrated in Fig. 1.

For reliability considerations it is essential to know the exact limits of the selected method of attachment; therefore, in addition to calculations, photoelastic investiga-

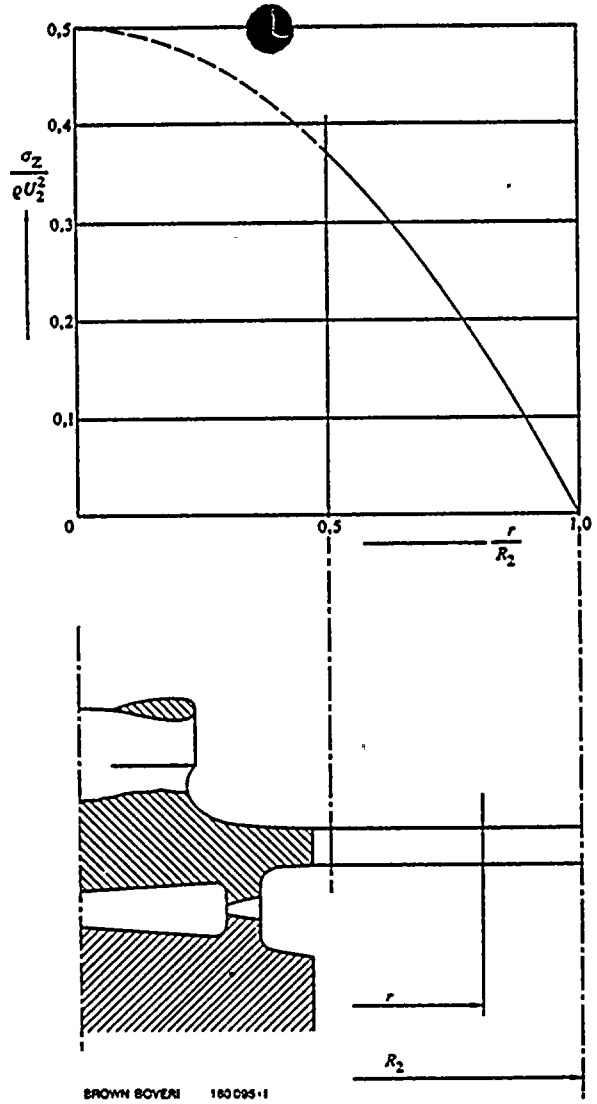

Fig. 5 – Stress distribution in a last-stage blade with constant cross-section

ϱ = Specific mass of the blade material
U_2 = Peripheral speed at blade tip

Other notation see Fig. 4.

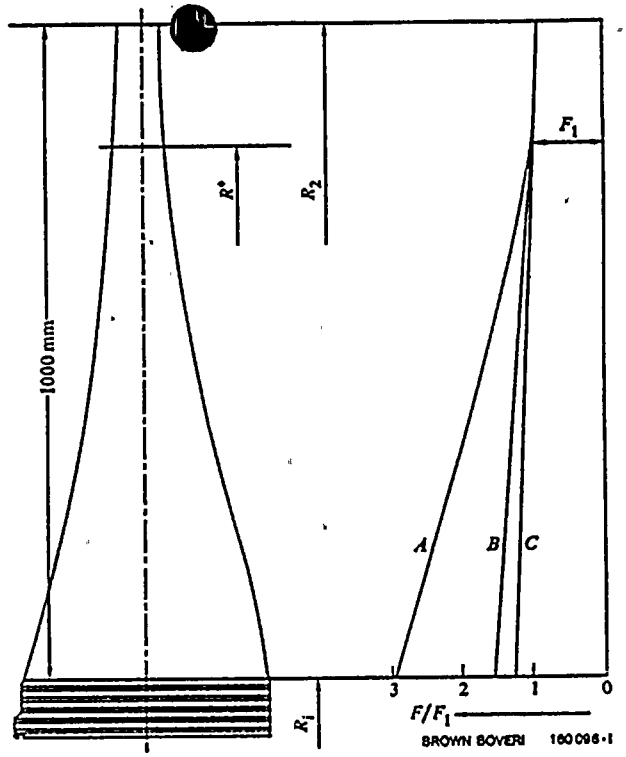

Fig. 6 – Variation of cross-sections of a blade given by equation (5) for different types of material

A = Steel
B = Titanium
C = Fibre-reinforced plastic
F = Cross-section

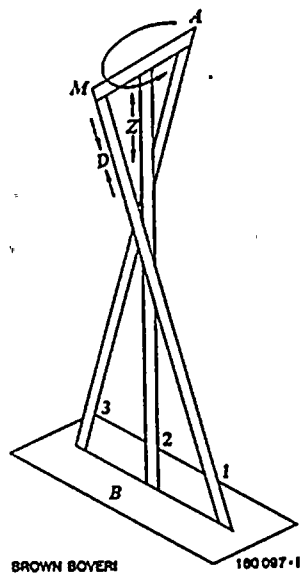

Fig. 7 – Model to explain unwinding stress

A = Blade tip
B = Fixing
D = Pressure
M = Torsion
Z = Tension
1 = Leading edge
2 = Central element of the cross-section
3 = Trailing edge

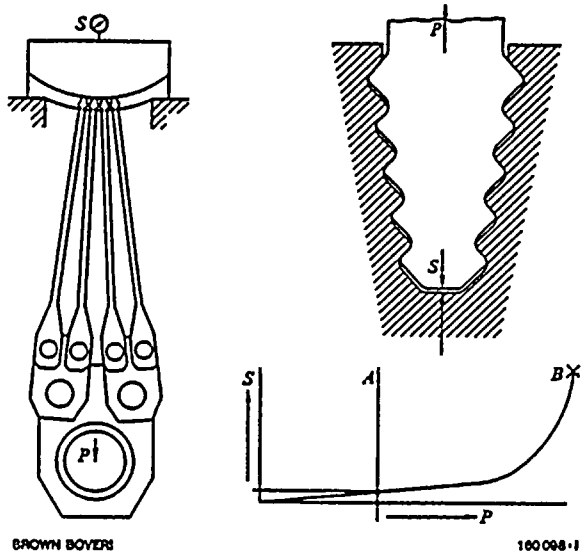

Fig. 8a – Pull-out test on a bent fir-tree root, with deformation diagram

A = Working point (rated speed)
B = Fracture
P = Tension
S = Clearance at the bottom of the groove, varying with tension

tions and pull-out tests on dummy blades are normally performed. Fig. 8 is a schematic illustration of such a test bed on which Brown Boveri perform full-scale tests up to a force of 2000 t. In the course of these tests not only the curve of deformation against force was plotted but also the notch stress at the bottom of the indentation in the fir-tree root. Using strain gauges with a grid of 0·4 mm local deformation was determined exactly to within a few per cent.

Effective Vibration

The last-stage blade is subjected to forced vibration when running; the sources of disturbance are listed in Table I. The magnitude of the forces acting on the blade in service is, however, largely unknown. Consequently, the results of calculations of the alternating stresses caused by the forced vibrations are open to considerable doubt. For this reason it has become normal practice to judge the mechanical quality of the blades according to the magnitude of the static stresses 1 to 5 (Table I) and the natural frequencies of the blade in relation to the exciting frequencies (multiples of the speed). With the aids to calculation that are available today the lower natural frequencies of the blade can be calculated sufficiently accurately to avoid

Fig. 8b – Rotor segment used for pull-out test

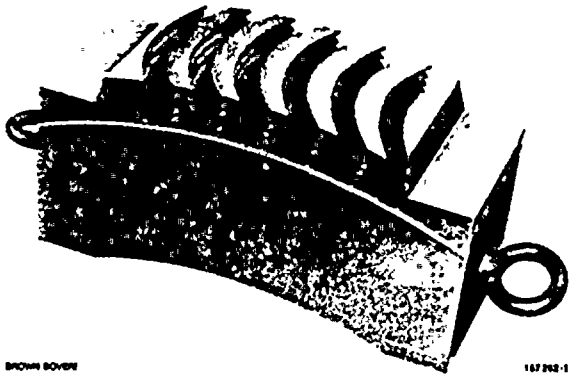

Fig. 8c – Blade root indentations sheered off in pull-out test

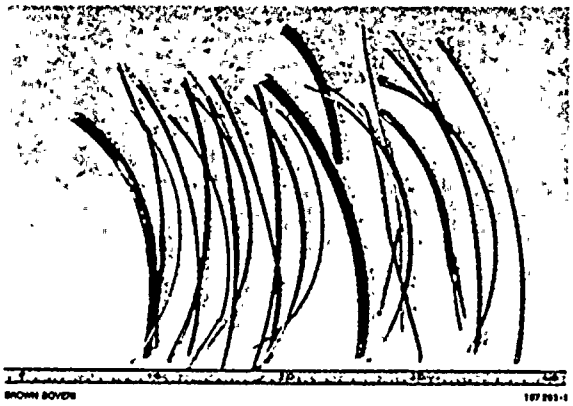

resonance with possible oscillating steam forces. Here, though, the following facts must be borne in mind.

– A decisive factor for assessing the vibration behaviour of the blade is its frequencies at operating speed. As can be seen in Fig. 9, the centrifugal force has a stiffening effect on the blade, with the result that the natural frequency increases with the speed of rotation. This rise is different for the various orders and depends on the shape of the oscillation. The stiffening effect is greater with flexural than with torsional vibration of the blade (see nodal lines in Fig. 9).

– Differences in material quality and tolerable deviations in geometry of individual blades result in a scatter band at each order of natural frequency.
– Simplifications and approximations which have to be taken into account when setting up a model for calculation result in discrepancies from reality.

For these reasons the calculation has to be recalibrated for the development of new blades whose shape differs from that of existing designs. The procedure adopted is roughly as follows:
Having calculated the first natural frequencies in terms of

Fig. 9 – Natural frequencies F of the blade plotted against speed n (rev/ min)

Nodal lines at the first four natural frequencies.

A, B, C, D = Permitted scatter bands of frequencies for zero speed measurement
$a, b, c, \ldots$ = Permitted scatter bands of blade frequencies at operating speed
E = Speed range in which the fixing rigidity is influenced by centrifugal force
G = Usual scatter band (precision forged blade)
H = Forbidden frequency range for measurements at zero and normal speed
n_s = Speed in rev/s
• = Values measured for zero speed vibration
——— = Values measured at different speeds

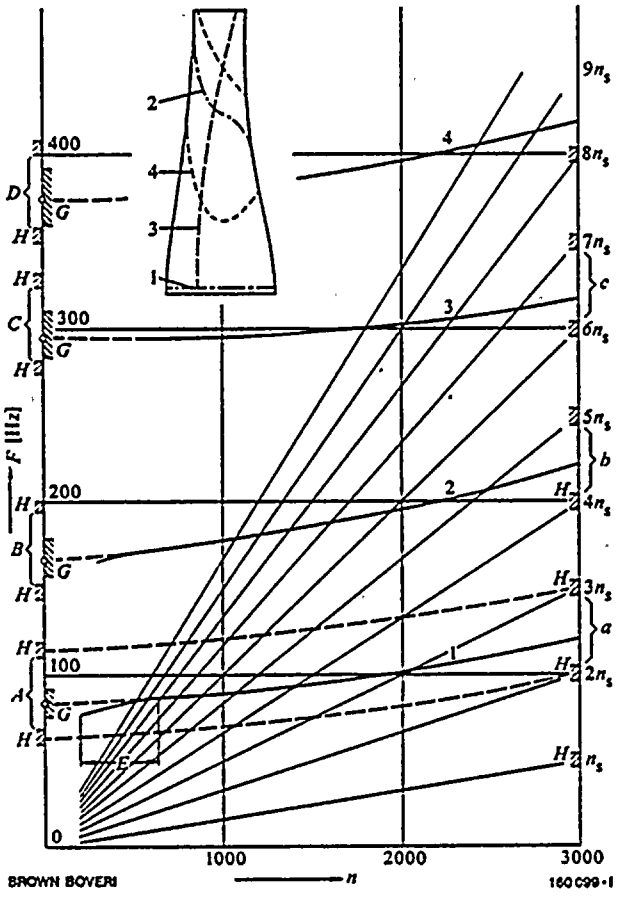

BROWN BOVERI 160 099-I

Fig. 10 – Arrangement of the telemetry system for measurement of vibration on last-stage blades in service

D = Strain gauge on the blade
W = Shaft
S = Transmitter
A = Pick-up ring

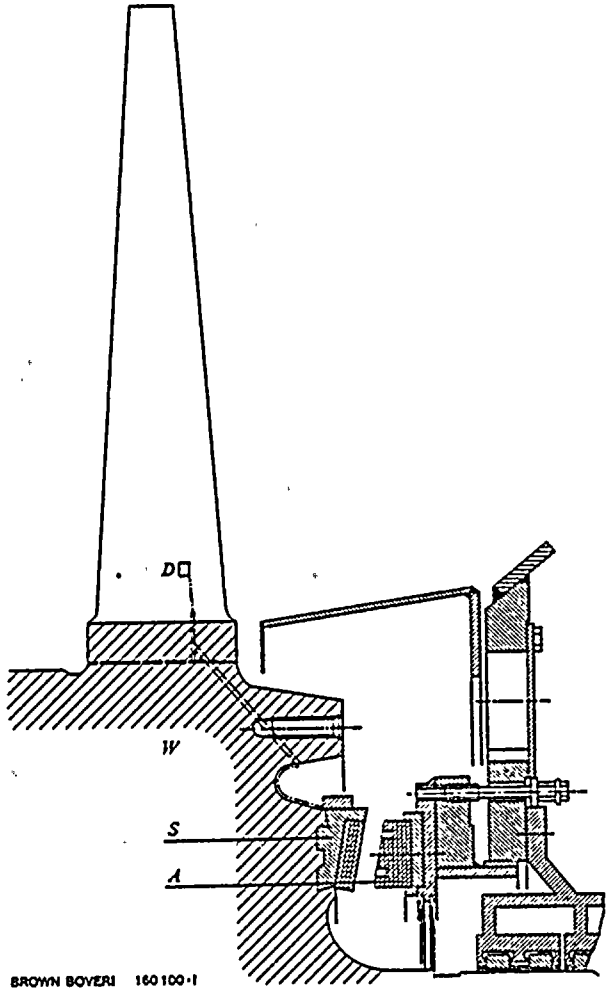

BROWN BOVERI 160 100-I

speed for blades with the desired dimensions and material qualities, each manufactured blade is checked at zero speed. By measuring the natural frequencies of some blades during overspeed testing it is possible to check whether the rise in frequency as a function of the speed was calculated correctly. Here the blade is made to vibrate by disturbance forces (excitation plates) many times larger than the disturbance forces actually experienced in service.
On completion of this test which has to be carried out once for every prototype last-stage blade, an economic selection of the manufactured blades can be performed by checking at zero speed ($n = 0$) alone. In Fig. 9 the frequency ranges *a*, *b*, *c*... are permissible at service speed, the range *H* is forbidden. Thus the permitted frequency ranges *A*, *B*, *C* at zero speed are fixed. To a limited extent completed blades whose routine zero speed measurement produces natural frequency values outside the ranges *A*, *B*, *C* can be brought inside these ranges by subsequent machining within the dimensional tolerance. However, it must be remembered that this subsequent machining changes all the natural frequencies.
The series of tests is concluded by measurements in service. In 1968 Brown Boveri checked a 600 MW machine by telemetry and was able to establish the dynamic behaviour of last-stage blades 1000 mm long throughout the entire load range. The main obstacles were the development of a watertight and erosion proof means of sticking and covering the strain gauges and the development of electronic equipment capable of withstanding centrifugal accelerations up to 7000 *g* and temperatures up to 150 °C for long periods. Fig. 10 shows the measuring set up. These measurements were repeated successfully in 1969 and 1971 on a 300 MW machine in which the steam had a high moisture content. Such measurements are nowadays desirable for various reasons and are gaining in significance because:

– Little is known about the stimulation which causes the blade to vibrate in service.
– The length of the blades in the last stages of steam turbines has been increased in recent years by all manufacturers and will continue to increase as unit outputs are raised. This will make the blades flexurally softer and they will respond to external influences by more pronounced vibration.
– In many places today the use of river water for cooling the condensers is no longer permitted. The use of cooling towers, however, results in warmer cooling water and consequently a higher pressure in the condenser compared with the fresh water cooling. Therefore, it is necessary to check whether the forces to which the final-stage blades are exposed as a result of the higher exhaust pressure do not represent an unreasonable strain.

During such measurements the following operational conditions were examined:
– While the machine was running up, the resonance of the blades (damping) was tested. The vacuum was varied between 30 and 250 mbar.
– The vibration of the final-stage blade was examined at different loads and exhaust pressures up to 250 mbar.
– By means of shutdown tests with partial and full vacuum breakage the behaviour of the final-stage blades was also tested under these abnormal conditions.

Fig. 11 shows the arrangement of the strain gauges on one of the blades examined. It was important to attach the strain gauges at points where there was a relatively high amplitude of vibration in order that the result of measurement at such points could be compared with the results of calculations and so that conclusions could be drawn regarding the maximum stresses to which the blade was subjected.

Fig. 11 – Strain gauges No. 51, 52, 53, 61, 62 and 63 on the rear of a test blade for measuring natural frequencies in service

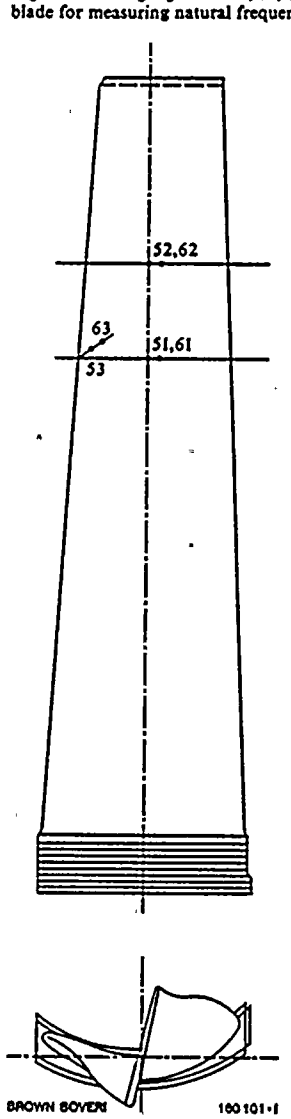

The results of these measurements can be summarized as follows:

- The blades are sufficiently proof against vibration fracture but only when the natural frequencies are not multiples of the speed of rotation.
- The aerodynamic excitation forces are very small provided steps are taken to avoid obvious sources of disturbance when designing and manufacturing the turbine.
- The excitation forces resulting from errors in the pitch of the stationary blade segments or of the actual stationary blades themselves, occur at such high frequencies that they do not represent a direct hazard for the blades.
- If the above requirements are taken into account, the maximum alternating stresses throughout the entire operational range and at the exhaust pressures in use nowadays are only a fraction of the strength of the blade material.
- At high exhaust pressures the amplitudes of vibration may be expected to increase. They are highest at no load, because here the aerodynamic conditions are unfavourable for the blades. For that point on the blade which is most severely stressed, alternating stresses may occur which reach such a high level in relation to the fatigue strength of the blade material, even in good designs, that they can no longer be ignored. Fig. 12 gives some idea of the vibration of the blades during a shutdown with full vacuum breakage. Therein the increase in the exhaust pressure p against time t can be seen, also the resultant drop in speed n of the shaft due to increased ventilation, the curve of the temperature T in the exhaust area as well as the curve of the natural frequency F and the amplitude A of the blade vibration at point 63 in Fig. 11.

Fig. 12 – Measurement of blade vibration during run-out of the machine following full vacuum breakage

F = Natural frequency of the test blade
A = Amplitude measured by strain gauge No. 63 in Fig. 11 at frequency F
T = Temperature in exhaust region
n = Speed of the turbine shaft
p = Pressure in exhaust region
t = Time

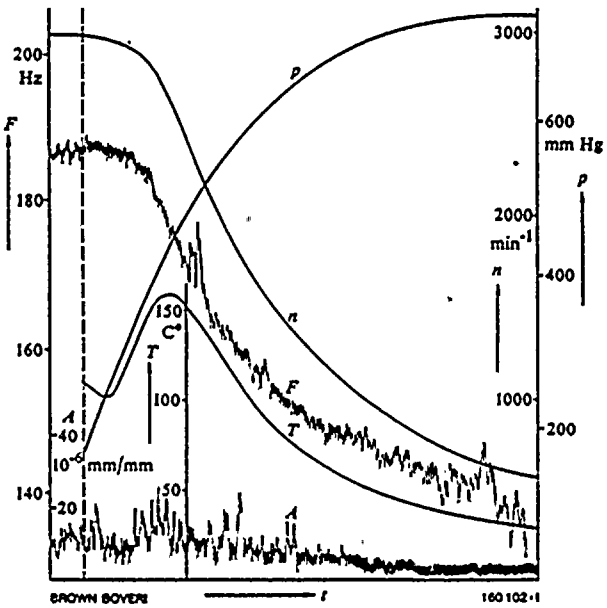

Fixing and Damping

In the discussion of blade vibration the question often arises regarding the influence of the flexibility of the blade fixing and of the damping on the vibration of the blade.
Owing to the enormous centrifugal forces acting on the blade in service, amounting to some hundreds of tons, the contact surfaces between the blade and the shaft are pressed against one another so strongly that not the slightest movement can occur at these points and therefore there is no variation in the natural frequencies of the blade which may be regarded as rigidly mounted. However, the indentations in the shaft and the foot of the blade have their own elasticity values which diverge from the rigid, ideal case. As can be seen in Fig. 13, this influence on the natural frequency of the blade is negligibly small, because current designs possess rigidity values which come fairly close to the absolutely rigid fixing [2].
The damping is composed of components which depend on the method of root fixing, the ambient medium and the material from which the blade is made. In practice this damping is measured by recording the logarithmic decrement. As Fig. 14 shows, the damping changes with the amplitude of the alternating stress. At stress values which can in fact occur in turbines, it reaches an order of magnitude at which a distinct change in the resonant frequency can be detected.

Erosion

The last stages of large condensing turbines operate in the wet steam region, where the steam contains 5 to 12% moisture. Mainly responsible for erosion is the water which separates out in the outermost third of the last row of stationary blades. Drop by drop this water is torn off

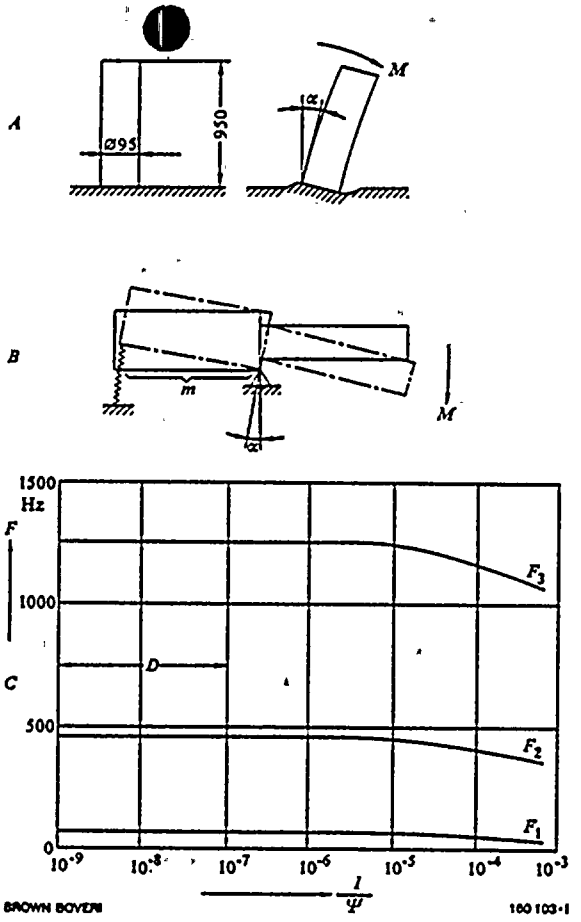

Fig. 13 – Influence of the elasticity of the blade fixing on the natural frequency

A = Fixing in the half plane

Rigidity of fixing $\Psi_1 = \frac{M}{\alpha} = 10^9$ kpcm

Young's modulus $E = 2{\cdot}1 \cdot 10^6$ kp/cm²

B = Theoretical equivalent fixing model $\Psi_2 = \frac{M}{\alpha}$

m = Rigid equivalent fixing with zero mass
α = Inclination at point of fixing due to M
C = Curve of frequencies F against fixing rigidity
F_1, F_2, F_3 = Natural frequencies of first to third order
D = Rigidity of common kinds of blade fixings

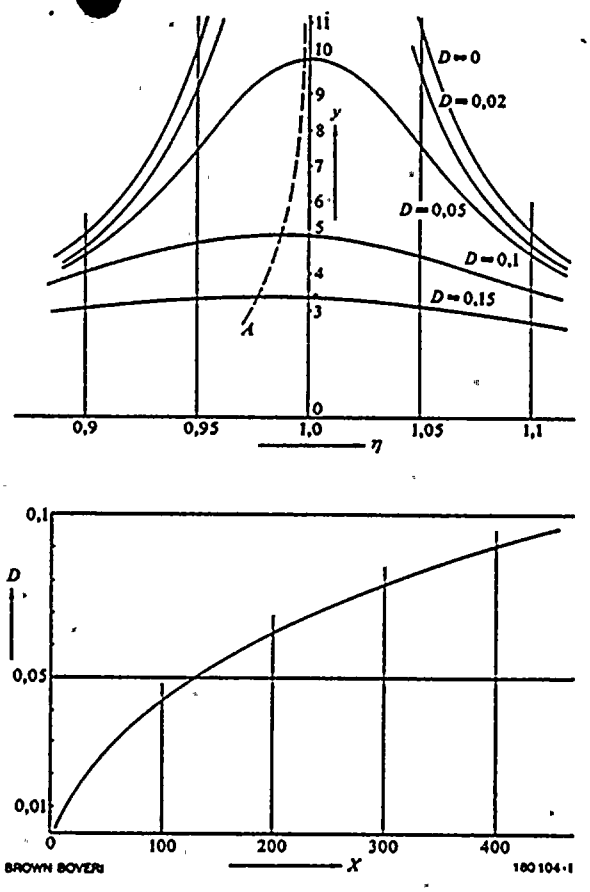

Fig. 14 – Incremental function and damping of a vibrating blade

y = Incremental function
η = Frequency ratio: Exciting frequency to resonant frequency
D = Lehr's coefficient of damping

Logarithmic decrement $\delta = \frac{2\pi D}{\sqrt{1-D^2}}$

X = Amplitude of alternating stress (kp/cm²)
A = Displacement of the peak frequency for $y = [y(\eta)]_{max}$ due to damping

the trailing edge of the stationary blades and accelerated by the flow of steam. The drops, which may be up to 0·2 mm across, reach velocities in the space between the stationary and moving blades which differ considerably from those of the steam flow [3]. This implies that there is a relatively large difference between the peripheral speed of the blade tip and the peripheral component of droplet speed, as a result of which the droplets strike the leading edge of the blade with an abrasive effect known as erosion.

Turbine manufacturers protect blades against erosion by armouring the leading edge. This can be done either by hardening the basic material (the method adopted by Brown Boveri) or by soldering on plates of Stellite.

The total amount of material lost by erosion is a logarithmic function of time; whereas the erosion rate is high during the initial period of service, it almost ceases after about one year [4]. An explanation for this is that the pores in the surface of the blade where erosion has taken place are partly filled with water, so that the impact forces of the drops striking the blades are only transferred to the material in a damped form (Fig. 15).

Future Prospects

It is the size of modern power station turbines which is their most impressive feature. Machines with unit ratings of over 1000 MW are being built; they have a total length of about 70 m, the diameter of the rotor measured across the tips of the final-stage blade varies between 4·5 and 5·5 m, depending on the manufacturer, while the casing surrounding the low-pressure rotor is almost as big as a private house. Since the trend toward further increases in unit capacities is continuing steps are already being taken to develop last-stage blades to even larger sizes in order to cope with the enormous steam volumes—in a 1100 MW machine the amount is about 30000 m³/s with a condenser vacuum of 0·05 bar—in a reasonable number of flows.

Here the stresses to which the rotor is subjected are of particular significance. Since the rotor discs are made of material whose yield point cannot be extended much further, an attempt is made to enlarge the outlet area by reducing the speed of the rotor and by employing a suitable material for the last-stage blades. Since, in current designs, the centrifugal forces of the last-stage blades

Fig. 15 – Eroded leading edge of a blade

Magnification 20×

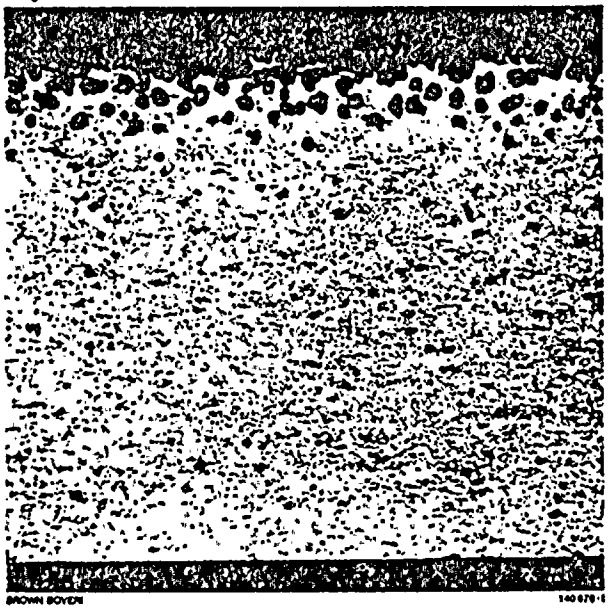

Fig. 16 – Carbon fibres before being inserted in the plastic matrix

Magnification 450×

produce stresses in the section of the rotor, which may amount to 35% of the total rotor stress, the general trend is towards blade materials with higher strengths but a lower specific weight. Foremost among such materials is titanium.

In recent years, however, reinforced materials (plastics) have found new fields of application. Among them, plastics reinforced with boron and carbon fibres exhibit properties which are quite equal to those of a high-alloy steel. The plastic blade therefore has a certain chance of being employed at the cold end of power station turbines, provided the very severe problem of erosion can be overcome. Table II shows the properties of a material of this kind. The carbon fibres embedded in the matrix have a diameter of about $5 \cdot 10^{-3}$ mm. Fig. 16 and 17 respectively show such fibres before being inserted in the plastic matrix and the surface of a fracture through such a composite bar.

The large steam turbines being built today are normally employed as base-load machines and they are expected to obtain a very high availability. As it is understandable that the individual elements have to be carefully examined even in the design stage, we make every effort to utilize modern computer and test facilities as far as possible. The aim of all these efforts is to ensure that future large machines with ratings above 1000 MW will be just as reliable and compact. In the attainment of this aim size and quality of the last-stage blades plays an important part.

Table II: Properties of a plastic material reinforced with carbon fibres

Matrix:	Epoxy resin		
Fibre:	Carbon (60% by volume)		
Density		1·6	g/cm³
Tensile strength	Longitudinal	7500	kp/cm²
Young's modulus	Longitudinal	$2 \cdot 4 \,..\, 10^{6}$	kp/cm²
Heat transfer coefficient	Longitudinal	34	W/m °C
	Transverse	2·9	W/m °C
Coefficient of thermal expansion	Longitudinal	$-0 \cdot 7 \,.\, 10^{-6}$	/°C
	Transverse	$28 \,.\, 10^{-6}$	/°C

Fig. 17 – Fractured surface of a compound material employing carbon fibre reinforcement

Magnification 1100×

Bibliography

[1] *J. Montoya Garcia:* Coupled bending and torsional vibrations in a twisted, rotating blade. Brown Boveri Rev. 1966 *53* (3) 216–230.

[2] *F. Vogt:* Über die Berechnung der Fundamentdeformation. Published by Norske Videnskaps Akademi, 1925.

[3] *G. Gyarmathy:* Grundlage einer Theorie der Nassdampfturbine. Mitteilung Nr. 6 published by the Institute for Thermal Turbo-Machines, Swiss Federal Institute of Technology, Zurich.

[4] *J. Hossli:* Problems in the construction of turbines for nuclear power plants. Brown Boveri Publication 3340 E (1967).

[5] *A. Hohn, P. Novacek:* Die Endschaufeln grosser Dampfturbinen aus mechanischer Sicht. Schweiz. Bauztg 1970 *88* (30) 673–678.

BBC
BROWN BOVERI

BBC Brown, Boveri & Company, Ltd., CH-5401 Baden/Switzerland

Printed in Switzerland (7812-750-0)
Classification No.0101